Available online at www.sciencedirect.com
SCIENCE DIRECT
Astroparticle Physics 25 (2006) 33–40
Astroparticle Physics
www.elsevier.com/locate/astropart

A second level trigger for the PAMELA satellite experiment

The PAMELA Collaboration

S. Orsi [a,*], J. Lundquist [a,1], M. Boezio [b], V. Bonvicini [b], P. Carlson [a], J. Lund [a], A. Menicucci [c,2], E. Mocchiutti [b], M. Pearce [a], P. Picozza [c], A. Vacchi [b], G. Zampa [b], N. Zampa [b]

[a] *The Royal Institute of Technology (KTH), Department of Physics, Albanova University Centre, SE-10691 Stockholm, Sweden*
[b] *INFN Laboratories, via A. Valerio 2, 34127 Trieste, Italy*
[c] *INFN, Structure of Rome II and Physics Department of University of Rome "Tor Vergata", Via della Ricerca Scientifica 1, I-00133 Rome, Italy*

Received 26 August 2005; received in revised form 4 November 2005; accepted 4 November 2005
Available online 1 December 2005

Abstract

The PAMELA space experiment will be launched on-board of a Russian Resurs DK1 satellite towards the end of 2005. The main scientific goal is the study of the antimatter component of the cosmic radiation. Three years of data taking will provide unprecedented statistics for antiprotons (80 MeV–190 GeV) and positrons (50 MeV–270 GeV) and will set the upper limit for the ratio $\overline{\mathrm{He}}/\mathrm{He}$ below 10^{-8}. PAMELA is built around a permanent magnet silicon spectrometer, surrounded by a plastic scintillator anticoincidence shield. An electromagnetic calorimeter is used for particle identification and energy measurements. If PAMELA data exceed the storage allowance on the satellite or the daily downlink quota (20 GB), a second level trigger may be activated by uplink from ground. Information from the anticoincidence system and from the calorimeter will be included in the second level trigger condition, providing a selective reduction of data. The second level trigger condition provides a reduction of data of ~60%, with a maximum systematic uncertainty in the proton (electron) spectra of 10% (3%). This uncertainty will be assessed during flight measuring one event every 10 without the second level trigger condition.

Keywords: Antimatter; Cosmic rays; Space experiment; Second level trigger; Antiprotons; Positrons

1. Introduction

The PAMELA satellite experiment (a Payload for Antimatter–Matter Exploration and Light-nuclei Astrophysics) [1,2] will be hosted onboard a Resurs DK1 satellite, orbiting the Earth at an altitude varying between 300 km and 600 km. The main scientific aim of PAMELA is the study of the antimatter component of the cosmic radiation above the atmosphere. PAMELA and its data acquisition system are described in Sections 2 and 3. In case the amount of data generated by PAMELA exceeds the storage allowance on the Resurs satellite or the daily downlink volume, a second level (L2) trigger can be activated from ground. Simulations have shown that the majority (~75%) of triggers in space are expected to be false triggers, i.e. where the coincidental energy deposits in the trigger scintillators are generated by secondary particles, produced in the mechanical structure of the experiment. The aim of the L2 trigger is to discard as many false triggers as possible, whilst rejecting a minor fraction of the good trigger events (i.e. the clean passage of a particle through the acceptance of PAMELA). Section 4 provides an overview of the trigger environment in orbit, in which particle fluxes and trigger rates are illustrated. The results from simulation studies of the expected proton and electron fluxes in orbit are

* Corresponding author. Tel.: +46 855378217; fax: +46 855378216.
E-mail address: silvio@particle.kth.se (S. Orsi).
[1] Now at INFN Laboratories, via A. Valerio 2, 34127 Trieste, Italy.
[2] Now at AGFA, Belgium.

0927-6505/$ - see front matter © 2005 Elsevier B.V. All rights reserved.
doi:10.1016/j.astropartphys.2005.11.001

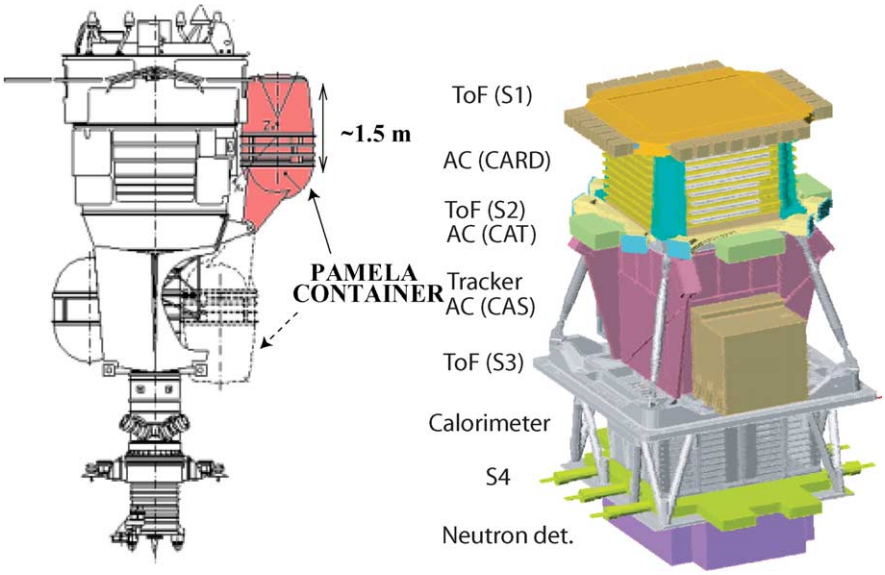

Fig. 1. Left: The PAMELA container is attached to the Resurs-DK1 satellite (~10 tonnes). The container is shown in acquisition position (shaded box) and in the rest position for launch and orbital maneuvers. Right: The PAMELA experiment is ~1.2 m high and weighs ~450 kg (750 kg with its container). From top to bottom, the apparatus consists of a time of flight system (S1, S2, S3 scintillator planes), an anticoincidence (AC) shield system (CARD, CAT, CAS scintillators), a magnetic spectrometer (tracker), an electromagnetic calorimeter, a shower tail catcher scintillator (S4) and a neutron detector. The electronics boxes attached to the sides of the experiment are not shown for clarity.

compared to experimental particle beam data. These studies show that good trigger events are often accompanied by backscattering from the calorimeter into the anticoincidence system. The second level trigger condition is based on information from the anticoincidence system and from the calorimeter. Sections 5 and 6 describe the second level trigger and its implementation.

2. The PAMELA experiment

PAMELA is built around a permanent magnet spectrometer (tracker) [3] equipped with double-sided silicon detectors. The tracker is surrounded by an anticoincidence (AC) system [4] which can be used to reject particles not cleanly entering the PAMELA acceptance. The main anticoincidence system consists of 5 plastic scintillators read-out by compact photomultiplier tubes. Four of the scintillators (CAS) cover the sides of the magnet and one (CAT) covers the top of the magnet, and has a rectangular hole corresponding to the tracker acceptance. Each CAS (CAT) scintillator is 8 mm thick and is read out by 2 (8) photomultiplier tubes for redundancy. The AC data acquisition system registers the activity in the AC detectors within a time window of 1.28 μs around the trigger, with 80 ns time resolution. The system only stores binary 'hit' information. There is no measurement of the total deposited energy. Events with energy deposit larger than 0.5 mips[3] are classified as a 'hit'. The time window of 1.28 μs has been chosen to allow an overlap with the calorimeter self-trigger signal, which is issued a few hundred nanoseconds after the interaction of a particle [5]. Four additional AC detectors (CARD) surround the volume between S1 and S2 (Fig. 1, right). Only the 4 CAS detectors have been implemented in the second level trigger.

Below the tracker is the electromagnetic calorimeter [5]. It is made of 44 silicon sensor planes interleaved with 22 plates of tungsten absorbers, giving a total depth of 16.3 X_0 (radiation lengths) and 0.6 λ (interaction lengths). Each plane is divided into 9 large area devices, each 380 μm thick, for a total sensitive area of about 24×24 cm^2. Each plane is segmented into 96 large strips with a pitch of 2.4 mm, for a total of 4224 electronics channels, read-out as 4 independent blocks. The primary function of the calorimeter is to distinguish between electromagnetic and hadronic showers. It is also used for the energy measurement of electrons and positrons. The bottom scintillator (S4) and the neutron detector are placed below the calorimeter and measure highly energetic events not contained in the calorimeter, aiding separation between electromagnetic and hadronic showers.

The time of flight system (ToF) [6] consists of six layers of plastic scintillator strips arranged in three planes (S1–S3); S1 and S2 are placed above the tracker, and S3 between the tracker and the calorimeter. It measures the velocity of the incident particles, rejecting albedo (upgoing) particles, and acts as the main PAMELA trigger [7] by identifying coincidental energy deposits in the scintillators (S1&S2&S3). Other trigger configurations (e.g. S2&S3) are foreseen to be activated in regions with high particle fluxes (polar regions and radiation belts), where the S1 scintillators would be continuously saturated. The geometrical acceptance of the experiment for energies over

[3] 1 mip = energy released by a minimum ionising particle impinging with a 90° angle to the scintillator.

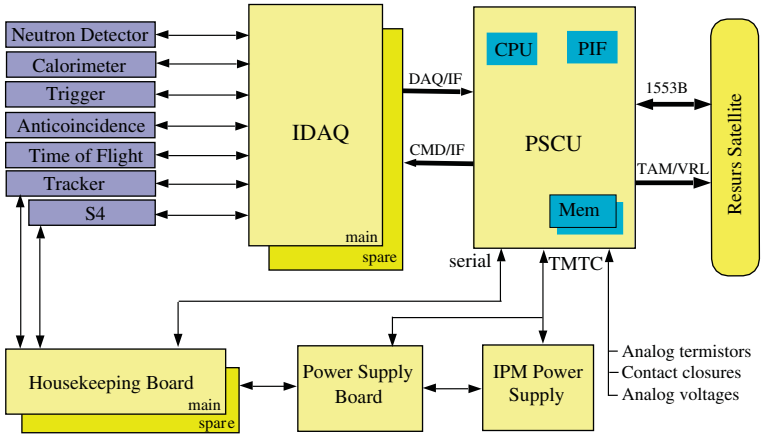

Fig. 2. Scheme of the PAMELA data acquisition system. The interfaces (IF) between the IDAQ and the PSCU handle the data acquisition and transfer the commands (CMD) to the IDAQ. The communication between PAMELA and the spacecraft is handled by the 1553B bus and by adapter modules for telemetry (TAM) and for data transfer (VRL). See description in Section 3. Adapted from [8].

10 GeV is determined by the geometry of the tracker cavity and is $\sim$20.5 cm^2 sr. At lower energies the intensity of the magnetic field bending particle trajectories becomes relevant and the acceptance decreases. In order to increase the PAMELA geometrical acceptance for electrons at energies above 300 GeV, a self-trigger feature is implemented in the calorimeter [5].

3. Data acquisition

The read-out system is illustrated in Fig. 2. The CPU of the experiment [8,9] (PSCU: PAMELA Storage and Control Unit) is based on a ERC-32 architecture (a SPARC v7 implementation) running a RTEMS real-time operating system. This custom-designed space qualified device is controlled by the satellite via a standard 1553B data bus. The PSCU handles all slow control, interaction with the satellite, data acquisition, storage and downlink. The PAMELA InterFace board (PIF) transfers data from the detectors to mass memory. Two redundant mass memory modules of 2 Gbytes each support latch-up detection; when a latch-up occurs, operation is transparently switched to the safe module. A multipurpose Telemetry and Control Board (TMTC) contains several interfaces to interact with the subsystems of the experiment.

Data acquisition from the subdetectors to the PSCU is performed via the Intermediate Data Acquisition System (IDAQ), at a rate of 2 Mbyte/s. When a particle enters the acceptance of the experiment and deposits coincidental energy in the ToF scintillators, the trigger front-end (FE) sends a trigger to the IDAQ. The PSCU, via the IDAQ, activates the procedure to sequentially read out the data from the subdetectors and to store them in the PSCU mass memory. Then, a few times a day, data are transferred into the satellite on-board memory (via a 10 Mbyte/s bus) and stored before being 'down-linked' to Earth. During each orbit, the satellite will send data to two downlink stations in Russia at a transmission rate of 150 Mbit/s. Two daily downlink 'windows' of about 10 min each will be dedicated to transfer PAMELA data to Earth, up to 20 GB/day. The possibility to up-link commands is present but limited, and will not allow real-time actions. This implies that semi-automatic procedures have to adopted to change the trigger mode and to take any action during flight.

The data acquisition system is dimensioned to handle the expected maximum data volume generated by PAMELA. The tracker, with its 36,864 channels, accounts for over 80% of the channels of the experiment, and therefore the event size depends mostly on the efficiency of the tracker data compression algorithm. The compression is based on a zero order prediction (ZOP) algorithm. The compression factor is estimated at 95%, with no degradation of the detector response [10]. The calorimeter data (4224 channels) are reduced by 80% through a pedestal suppression method. As we will discuss later, we expect an average trigger rate of $\sim$10 Hz and an average event size (compressed data) of 6 kB, which create a daily data volume of $\sim$5 GB. Applying a safety factor to this estimate, the acquisition system is designed to handle up to 20 GB/day. The main uncertainties are the limitation of the GEISHA [11] hadron shower Monte Carlo used in the simulations and the unknown effect on the trigger rate of particle interactions in the satellite structure. The simulations presented in this work refer to particle interactions with the mechanical structure of PAMELA and its container, while the satellite is not present in the simulated mechanical model. Even if PAMELA is positioned on the side of the satellite, and therefore the good trigger rate will not be affected by particle interaction in the mechanical structure of the satellite, the false trigger rate may be affected. This effect will be quantified using flight data. If the amount of data exceeds either the storage allowance dedicated to PAMELA on the Resurs spacecraft or the daily limit of 20 GB of data down-linked to ground,[4] an online event

[4] This is not a technical limitation of the experiment, that can continuously acquire data up to a trigger rate of $\sim$60 Hz, generating more data than the mentioned quota of 20 GB.

selection can be applied through a second level (L2) trigger, to be activated by an uplink command from ground.

4. Trigger environment

The interaction of protons with the PAMELA apparatus has been simulated over a wide energy range. The expected proton flux for PAMELA is evaluated making use of AMS-01 [12] data. Since the orbital inclination for PAMELA is larger than that of AMS-01 (70.4° and 51.7°, respectively), the flux at high geomagnetic latitudes, where experimental data are not available, has been assumed not to depend on the geomagnetic latitude (top line in Fig. 3). This assumption is justified by comparing AMS results with cosmic ray proton flux measurements in quasi-polar regions [13,14]. Fig. 3 shows a comparison of PAMELA expectations and AMS-01 data for one orbital period. Heavier nuclei and electrons, that constitute, respectively, ~9% and ~1% of particles in space, have not been included in the comparison. This results in an estimated discrepancy between this analysis and the flux in orbit of the order of 10%. The expected differential proton trigger rate for PAMELA for good triggers (t_g), false triggers (t_f) and total ($t_t = t_g + t_f$) are shown in Fig. 4. Fig. 5 shows a visual representation of good triggers (with and without activity in the AC system) and false triggers. The total trigger rates are obtained by integration over the simulated kinetic energy range ($E_{min} = 82$ MeV, $E_{max} = 100$ GeV):

$$T_x = \int_{E_{min}}^{E_{max}} t_x(E)\,dE, \tag{1}$$

where $x = t, g, f$. Calculations lead to the expected rates: $T_g = 2.0$ Hz, $T_f = 6.5$ Hz, $T_t = 8.5$ Hz. Fig. 6 shows the expected trigger rate as function of the orbital position. Apart from the South Atlantic Anomaly (SAA), the expected trigger rate is always lower than the maximum trigger rate PAMELA is designed to manage (~60 Hz).

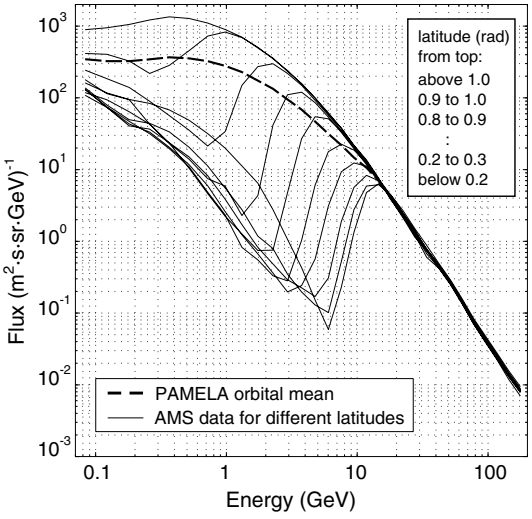

Fig. 3. Expected down-going cosmic proton spectrum for PAMELA averaged on one orbit (bold line). The proton spectra measured by AMS-01 [12] on-board the Space Shuttle for several geomagnetic latitudes are shown for reference. During its test flight, AMS-01 orbit (geographic) had an inclination of 51.7°, while PAMELA will fly on a quasi-polar orbit (70.4°).

4.1. Backscattering studies

Studies to discriminate backscattering events from false triggers have been performed using beam particles (elec-

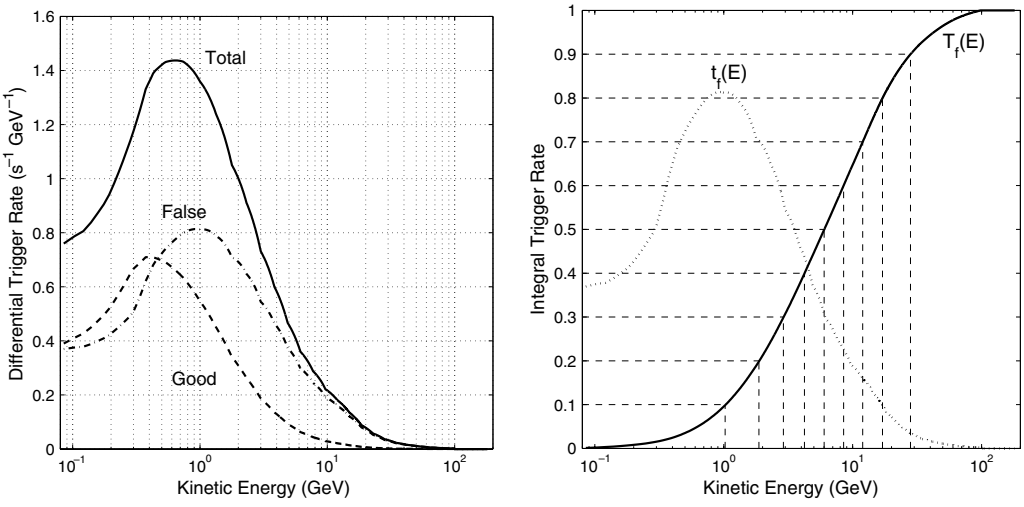

Fig. 4. Left: The simulated expected differential trigger rate shown as a function of the kinetic energy of the incoming proton for good triggers (dashed line), false triggers (dash-dot) and total (good + false, solid line). The plot contains simulated cosmic protons, averaged over one orbit (Fig. 3). Right: The integrated false trigger rate averaged over one orbit and normalised to unit area. Regions separated by the dashed lines contain 10% of the total false triggers. Particles with energy in the range 1–28 GeV cause 80% of the false triggers. To significantly reduce the amount of data, the L2 condition must have a large rejection ratio (rejected false triggers divided by total false triggers) in this energy range. The differential false trigger rate is shown for reference (dotted line).

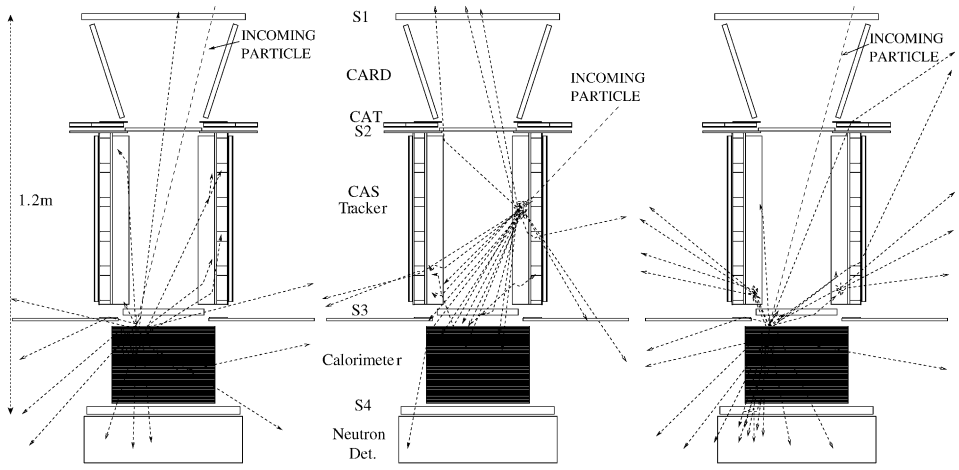

Fig. 5. Visual representation of simulated proton interaction in the experiment. Left: Good trigger event without activity in the AC detectors. A particle entering the tracker cavity from the sides may give rise to particle showers that trigger the experiment (false trigger, centre). Since the cosmic ray flux consists mainly of protons and light nuclei, the induced shower is likely to be predominantly hadronic. False trigger events are often characterised by activity in the AC detectors, as are good trigger events with backscattering from the calorimeter (right).

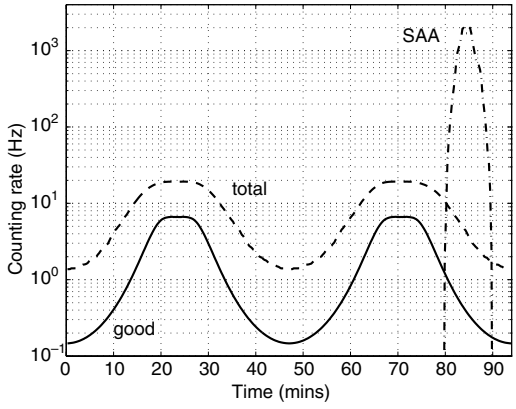

Fig. 6. The PAMELA trigger rate evaluated during an arbitrary orbit (period ~94 min). The dotted curve is an estimation of the total trigger rate, while the lower curve shows only the good triggers. The trigger rate is strongly dependent on the orbital position, and reaches a minimum in equatorial regions. The sharp increase in the trigger rate towards the right of the plot is due to the South Atlantic Anomaly (SAA). Adapted from [15].

trons, protons and pions) from the PS and SPS accelerators at CERN. The data have been compared to Monte Carlo simulations performed with GPAMELA [16], which uses the GEANT 3.21 package [17] to simulate particle interactions within PAMELA. The GEISHA hadron shower Monte Carlo is used to simulate the interactions of hadrons with the nuclei of the traversed matter.

The backscattering from the calorimeter for particles traversing the scintillators S1, S2 and S3 and entering the magnet cavity has been investigated. The backscattering ratio in the CAS detectors (the fraction of events with activity in at least one CAS detector) is proportional to the activity in the calorimeter, which is dependent on the particle energy and type. Fig. 7 shows the backscattering ratio for electrons and protons in the CAS detectors measured during a beam test at the SPS in 2003, where PAMELA was assembled in the flight configuration. In each of the 5 plots, the five bins represent the backscattering ratio in each CAS detector separately (bins 1–4) and in at least one CAS detector (bin 5). The particle beam was displaced from the centre of the acceptance, which results in different backscattering ratio in the four detectors.

The experimental data from the beam tests have been compared to simulations in order to verify the validity of the GPAMELA Monte Carlo package. Fig. 7 shows a comparison of experimental and simulated data with test beam electrons and protons. While the backscattering prediction for electrons with energies of 20–180 GeV differ by less than 5% from the measured values, for protons the error is up to 50%. This result indicates limitations of the GEISHA hadron shower Monte Carlo. Fig. 7(right) shows that GEISHA predicts a systematically lower interaction multiplicity for backscattering compared to experimental results. The interactions within the calorimeter have been shown to be reproduced more accurately [18].

5. The second level trigger

The PAMELA experiment is expected to acquire data through-out its lifetime with the trigger conditions described in Section 2. Although the overall DAQ design is conservative, under special circumstances the transferred data volume from the satellite to ground may need to be reduced. The second level trigger has the task to selectively reduce the data to be transferred to ground by recognising and discarding as many false triggers as possible, at the expense of loosing only a minor fraction of the good events.

The majority of false triggers are due to particles with energies in the range from 1 to a few 10's of GeV, as shown by the bold line of Fig. 4(right), that represents the function $T_f(E) = \int_0^E t_f(E')\,dE'$. False triggers and good events

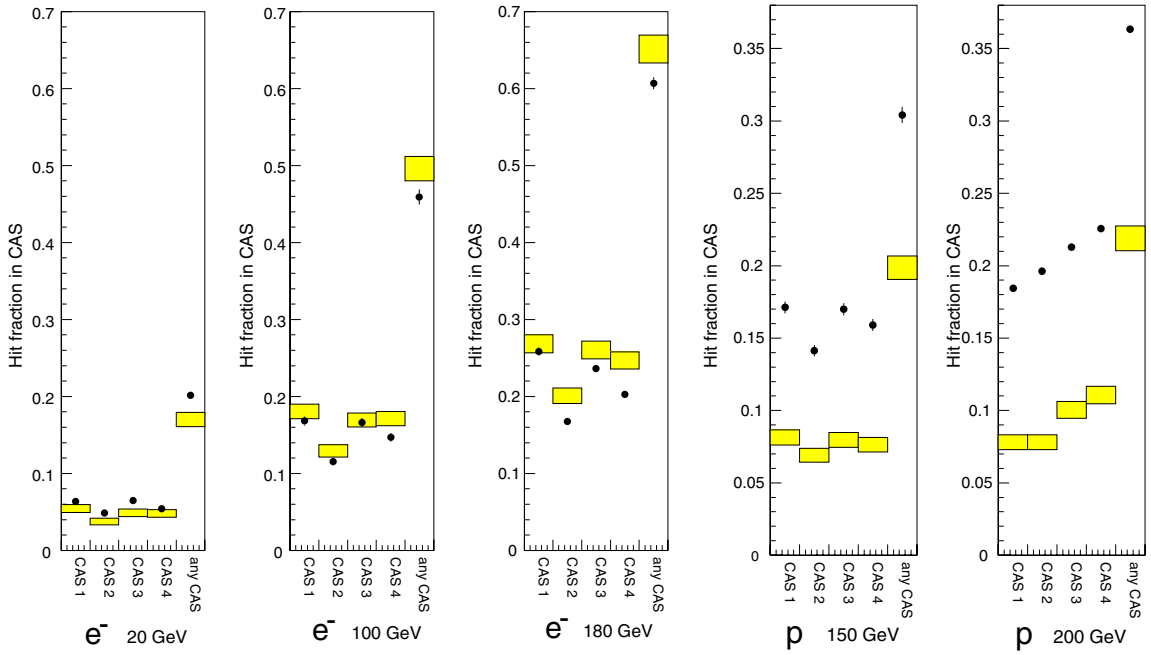

Fig. 7. Comparison of experimental data from beam test studies (filled circles, with statistical error bars) with simulations (shaded boxes, including statistical error bars). The fraction of events with activity in CAS detectors is shown for electrons (left) with energies of 20, 100 and 180 GeV, and for protons (right) with energies of 150 and 200 GeV. Differences in the beam trajectory through PAMELA between the 5 runs plotted here (always close to the centre of PAMELA acceptance) explain the relative differences between the 4 detectors.

with backscattering may be discriminated with an online analysis, since false triggers are likely to deposit less energy in the calorimeter compared to backscattering events. The second level trigger implemented in the experiment discards all the events characterised by activity in the AC system if the number of strips hit in each of the 4 sections of the calorimeter is lower than a given threshold ($n_s = 70$).

The rejection ratio $r_f(E, n_s)$ is defined as the number of rejected false triggers divided by the total numbers of false triggers. It is a function of the kinetic energy (E) of the incoming proton (for the false trigger simulations only protons were used) and of the number of calorimeter strips hit (n_s). Fig. 8 shows the dependance of $r_f(E, n_s)$ on the energy

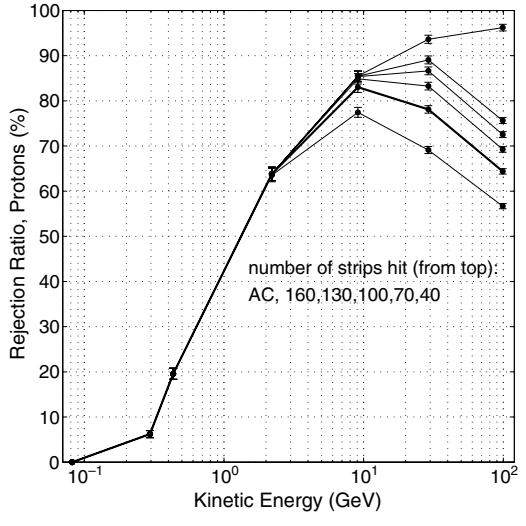

Fig. 8. The rejection ratio (fraction of false proton triggers correctly identified and discarded) as function of the kinetic energy of the incoming (simulated) proton. Each line corresponds to a different number of calorimeter strips hit. The top line represents the backscattering ratio, with no condition on the number of strips hit ($n_s = \infty$). The bold line corresponds to $n_s = 70$, which is the value adopted in the implementation of the L2 trigger.

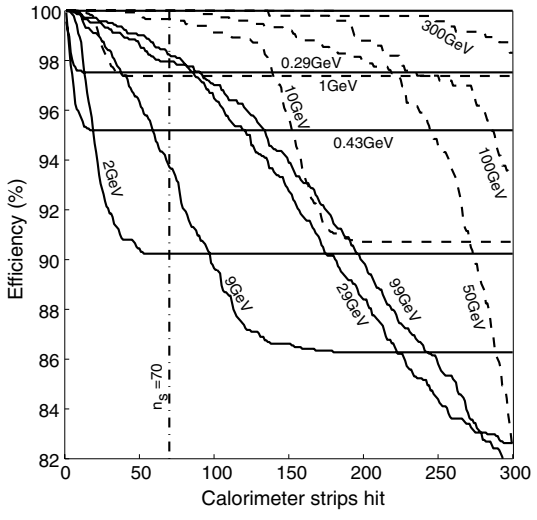

Fig. 9. The efficiency η of the L2 trigger is shown as function of n_s for simulated protons (solid lines) and electrons (dashed lines) of several energies. The efficiencies for the chosen value $n_s = 70$ (dash-dot line) correspond to the values shown in Fig. 10(bold line).

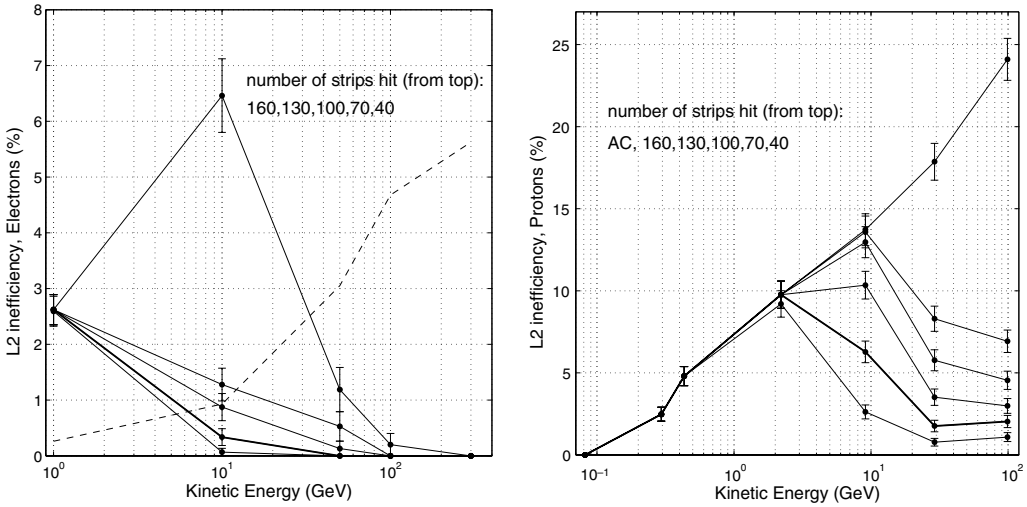

Fig. 10. Simulated good triggers with activity in the AC system (due to backscattering) and a condition on the number of calorimeter strips hit. Electrons (left, energy range 1–300 GeV) and protons (right, 82 MeV–100 GeV) are shown. With a condition on the maximum number of calorimeter strips hit, the backscattering ratio is strongly decreased for both electrons and protons. The plots represent the inefficiency, i.e. the fraction of good electron (proton) triggers lost (%) when the L2 trigger is active. The top line in the right plot represents the backscattering ratio, with no condition on the number of strips hit ($n_s = \infty$). The backscattering ratio for electrons for large n_s (500) is shown in the left plot, scaled by a factor 10^{-1} (dashed line), and ranges from 2% to ~60%. The bold lines correspond to $n_s = 70$, which is the value adopted in the implementation of the L2 trigger.

for a selected number of calorimeter strips hit. The chosen value $n_s = 70$ corresponds to a rejection ratio of 70–80% in the energy range 1–30 GeV. This threshold has been chosen to have a minimum efficiency η (fraction of good triggers correctly identified, Fig. 9) of 90%. Fig. 10 shows the expected inefficiency $1 - \eta$ for the same values of n_s shown in Fig. 8. The inefficiencies for electrons (left) and protons (right) are lower than 3% and 10%, respectively, over the whole spectrum ($n_s = 70$, bold lines). When the L2 trigger is active, one event in every 10 is recorded independently of the L2 condition, in order to build a sample of unbiased triggers and to monitor off-line the performance of the second level trigger. The inefficiency is a systematic error that will be determined off-line by using the unbiased trigger samples. The systematic error will be significantly lower[5] than the values of 10% for protons and 3% for electrons shown in Fig. 10.

The total rejection ratio is obtained by the convolution of $r_f(E,n_s)$ and $t_f(E)$:

$$R(n_s) = \frac{1}{T_f} \int t_f(E) r_f(E, n_s)\, dE \qquad (2)$$

and is estimated to be 70% for $n_s = 70$. This reduces the false trigger rate from 6.5 Hz to 2.0 Hz. The electronic noise in the calorimeter recorded during ground-based cosmic-ray runs is below $n_s = 40$. Considering electronic noise of $n_s = 40$, the total rejection ratio becomes 63% and the false trigger rate 2.4 Hz. Fig. 11 illustrates the cases with and without electronic noise.

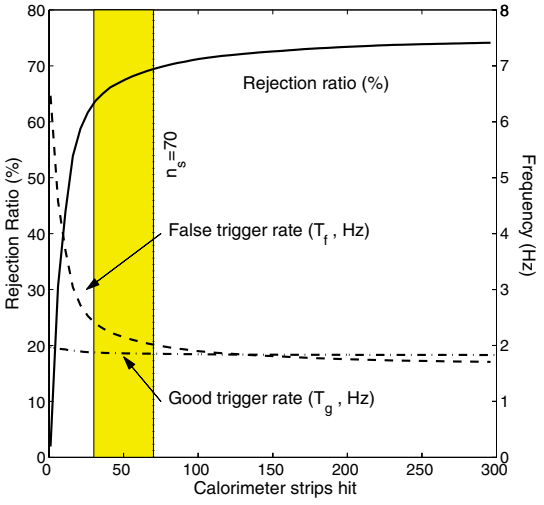

Fig. 11. The total rejection ratio (%) shown (solid line) together with the total false trigger rate (Hz) as function of the number of strips hit (n_s). The chosen value n_s corresponds to $T_f = 2.0$ Hz, $T_g = 1.9$ Hz. In the presence of electronic noise with signal in less than 40 strips (the shaded area represents the electronic noise measured in tests with the calorimeter) the trigger rates are expected to be $T_f < 2.4$ Hz, $T_g < 1.9$ Hz (values corresponding to $n_s = 30$ in the figure, without noise).

The L2 condition has been applied to selected runs with proton and electron beams[6] directed close to the centre of the PAMELA acceptance (good triggers). All electrons with energy of 40 GeV pass the L2 condition ($\eta = 100\%$), in good agreement with the simulations (Fig. 10, left). Only

[5] The systematic errors will be the statistical error bars shown in Fig. 10 for simulated events.

[6] Only data collected at the SPS accelerator were available, which makes a comparison between simulations and experimental data possible only in the higher part of the spectrum.

$2.0 \pm 0.2\%$ of the good proton triggers at 150 GeV ($2.38 \pm 0.05\%$ at 200 GeV) are rejected by the L2 condition, compared to $1.0 \pm 0.1\%$ for 150 GeV and $0.9 \pm 0.1\%$ for 200 GeV protons (Fig. 10, right). Systematic uncertainties were not taken into account in the error bars, which might explain the difference between simulation and experiment.

6. Implementation of the second level trigger

The second level trigger algorithm has been implemented on a digital signal processor (DSP) within the IDAQ and will be activated by the PSCU upon uplink commands from ground. The architecture of the IDAQ uses the DSP as a simple arithmetic and logic unit (ALU) and does not require any controller capabilities. This choice was taken because of the higher expected single event upset (SEU) rate (about 1 event per day) for the DSP compared to the controller Actel programmable logic array devices (less than 10^{-4} SEU per day) [19]. The DSP is a reprogrammable device, which makes the design flexible. During flight the software running on the DSP may be upgraded from ground via dedicated macro-commands that will uplink a small number of parameters in order to change the L2 condition.

When the second level trigger is activated, data are read out from the subdetectors to the IDAQ according to the selected trigger condition. The software running on the DSP checks the event by reading the words dedicated to the second level trigger in the AC and calorimeter subpackets. As soon as the event is found not to fulfill any of the conditions for rejection, the program releases the status flag. The IDAQ will then transfer the data packets to the PIF to store it into mass memory. If the event is recognised as false trigger, only a brief summary of the event is saved. The system is then ready for a new acquisition. In the case that the event data are malformed or any detector package is missing, the data relative to the event are saved into mass memory for offline analysis.

7. Conclusions

The PAMELA space experiment will acquire data during 3 years with coincidental energy deposits in the trigger scintillators used as the primary trigger. In case the amount of data exceeds the storage allowance on the Resurs satellite or the daily downlink volume, a second level trigger can be activated from ground. The L2 condition is based on information from the anticoincidence system and from the calorimeter. All events characterised by activity in the AC system and with less than 70 strips hit in the calorimeter are considered as false triggers and discarded. Simulations show that more than 70% of the false triggers are removed by the L2 condition (total data reduction ~60%). Only 7% of the good trigger events are discarded. For electrons the inefficiency is always less than 3% and decreases with energy.

One event every 10 is recorded using the main trigger condition, to monitor off-line the performance and efficiency of the second level trigger. This will allow a precise evaluation of the fraction of discarded good events, reducing the systematic errors significantly below the maximum expected 10% (3%) proton (electron) detection inefficiency.

Acknowledgements

The authors thank the PAMELA Collaboration for their support during the writing of this paper. In particular, we thank Alessandro Basili for information provided on the data acquisition system, Paolo Papini, Sandro Tassa and Fabrizio Sebastiani for the help with the DSP software and CPU programming and Samuele Straulino for the data used to produce Fig. 6. The KTH group thanks The Swedish National Space Board and The Swedish Research Council (VR) for financial support.

References

[1] M. Boezio et al., Nucl. Phys. B—Proc. Suppl. 134 (2004) 39.
[2] PAMELA homepage: <http://wizard.roma2.infn.it/pamela/>.
[3] O. Adriani et al., Nucl. Phys. B—Proc. Suppl. 125 (September) (2003) 308.
[4] S. Orsi et al., The anticoincidence shield of the PAMELA space experiment, in: Proceedings of the 35th COSPAR Scientific Assembly, Paris, France, 2004, Adv. Space Res., in press.
[5] M. Boezio et al., Nucl. Instrum. Meth. Phys. Res. A 487 (2002) 407.
[6] D. Campana et al., in: Proceedings of the 28th ICRC, Tsukuba, Japan, 2003, vol. 1, p. 2141.
[7] G. Osteria et al., Nucl. Instrum. Meth. Phys. Res. A 518 (2004) 161.
[8] M. Casolino et al., The PAMELA storage and control unit, in: Proceedings of the 35th COSPAR Scientific Assembly, Paris, France, 2004, Adv. Space Res., in press.
[9] F. Altamura et al., The central processing unit of PAMELA experiment, Frascati Phys. Ser. VVV (2004) 1.
[10] O. Adriani et al., The microstrip silicon magnetic spectrometer of the PAMELA experiment, in: Proceedings of the 26th ICRC (OG 4.2.10.), Salt Lake City, USA, 1999.
[11] H.C. Fesefeldt, Technical Report PITHA 85-02, Phys. Inst., RWTH Aachen.
[12] M. Aguilar et al., Phys. Rep. 366 (6) (2002) 331.
[13] M. Boezio et al., Astrophys. J. 518 (1999) 457.
[14] T. Sanuki et al., Astrophys. J. 545 (2000) 1135.
[15] S. Straulino, private communication.;
S. Straulino, Simulation of Silicon Microstrip Detectors for a Cosmic Ray Experiment, Ph.D. Thesis, Bologna, 2003. Available online at [2].
[16] Available from: <http://www.ba.infn.it/~ambriola/gpamela/>.
[17] R. Brun et al., Detector description and simulation tool, CERN Program Library, 1994.
[18] J. Lund, Antiparticle Identification Studies with the PAMELA Satellite Experiment, Ph.D. Thesis, KTH, Stockholm 2004. Available online at [2].
[19] M. Boscherini et al., Nucl. Instrum. Meth. Phys. Res. A 514 (2003) 514.